AIAA JOURNAL
Vol. 42, No. 1, January 2004

Optimum Design of Shell Structures with Stiffening Beams

Nikolaos D. Lagaros,* Michalis Fragiadakis,† and Manolis Papadrakakis‡
National Technical University of Athens, Athens 157 80, Greece

The optimum design of stiffened shell structures is investigated using a robust and efficient optimization algorithm where the total weight of the structure is to be minimized subject to behavioral constraints imposed by structural design codes. Evolutionary algorithms and more specifically the evolution strategies (ES) method specially tailored for this type of problems is implemented for the solution of the structural optimization problem. The discretization of the stiffened shell is performed by means of cost-effective and reliable shell and beam elements that incorporate the natural mode concept. Three types of design variables are considered: sizing, shape, and topology. A benchmark test example is examined where the efficiency and robustness of ES over other optimization methods is investigated. Two case studies of stiffened shells are subsequently presented, where a parametric study is undertaken to obtain the most efficient design compatible with the regulations suggested by design codes such as Eurocode. The important role of the stiffeners and how they can be optimally chosen to improve the performance of shell structures in terms of carrying capacity and economy is demonstrated.

I. Introduction

ANALYSIS of shell structures presents a challenge because their formulation may become cumbersome and their behavior can be unpredictable with regard to the geometry or support conditions. Although shell structures reinforced with beams exhibit enhanced structural behavior as opposed to nonstiffened shells, comparatively little attention has been given to this type of structure. The research work dealing with the optimum design of shell structures is rather limited,[1–7] and the optimum configuration of stiffened shells is an issue that has not yet been addressed adequately by the scientific community. Maute and Ramm[1] solved a material topology optimization problem where the design model is adapted during the optimization process. Lee et al.[2] presented a general methodology for topology optimization using an artificial material model to take into account the irregular distribution of material density of isotropic multilayer shell structures. Magnucki[3] proposed a design process for circular tanks, where the optimal geometric characteristics of such structures are investigated under the objective of minimal mass. Afonso et al.[4] presented a two-step procedure, where the optimal stiffening zones of plate structures are first identified followed by a sizing optimization to determine the dimensions of the stiffeners to minimize the strain energy under constant total volume. Akl et al.[5] presented a process for the design of underwater stiffened shell structures, where a multicriteria optimization approach is utilized to select the optimal dimensions and spacing of the stiffeners to minimize the shell vibration, the associated sound vibration, and the weight of the rings, as well as the cost of the structure. Farkas and Jarmai[6] introduced an analytical method of minimizing the cost of stiffened plates under hydrostatic pressure, whereas experimental results on the behavior and the failure modes of these structures are presented by Butler et al.[7] Note that all of the cited studies were based on gradient-based optimization algorithms.

The objective of paper is to present a reliable tool for the optimum design of realistic stiffened shell structures. When it comes to structural systems such as shells with stiffening beams, the designer must be able to estimate the position and the cross section of the stiffening beams in conjunction with the thickness and the geometry of the shell to obtain the best performance under given loading conditions. Rules imposed by design codes must also be taken into consideration by the optimization procedure to reach realistic optimum designs. On the other hand, the optimization algorithm must be robust, efficient, and as versatile as possible, neither dependent on the type of problem nor on the finite element formulation or the constraints of the design codes. The optimization method employed in this study is based on the evolution strategies (ES) method, which belongs to the evolutionary type of algorithms, and has been tailored to meet the specific characteristics of the problem at hand.

The test cases considered are combined optimization problems with three types of design variables: sizing, shape, and topology. The combined optimization problem is defined by the type of active design variables resulting to a sizing, a sizing–shape or a sizing–shape–topology optimization problem. A design variable is considered to be active when it is permitted to change its value, whereas in the case of a nonactive design variable, its value remains constant during the optimization process.

For the finite element (FE) discretization of stiffened shells, the natural mode triangular composites (TRIC)[8] shell element and the beam composites (BEC)[9] elements are used. Both elements, introduced by Argyris et al.,[8,9] have some desired features, such as robustness, accuracy, and computational efficiency, as shown elsewhere.[10,11] Because the optimization of shell structures is a computationally demanding task, it is imperative to use reliable and cost-efficient FE analysis to be able to optimize realistic shell structures.

The rest of the paper is organized as follows: A short presentation of the FE employed for the discretization of the shell and the stiffeners is given in Sec. II. Subsequently, the optimization problem is described in Sec. III, followed by an outline of the ES algorithm in Sec. IV. In Sec. V, the optimization problem of stiffened shells is described. In Sec. VI, a benchmark test, where the efficiency of ES over other optimization methods is examined, and two test examples are presented, to demonstrate the potential of the proposed approach in solving realistic optimization problems of stiffened shell structures.

II. Formulation of the Structural Optimization Problem

Structural optimization problems are characterized by various objective and constraint functions that are generally nonlinear functions of the design variables. These functions are usually implicit, discontinuous, and nonconvex. The mathematical formulation of structural optimization problems with respect to the design

Received 16 July 2002; revision received 3 July 2003; accepted for publication 5 August 2003.

*Research Associate, Institute of Structural Analysis and Seismic Research; nlagaros@central.ntua.gr.
†Ph.D. Student, Institute of Structural Analysis and Seismic Research; mfrag@central.ntua.gr.
‡Professor, Institute of Structural Analysis and Seismic Research; mpapadra@central.ntua.gr.

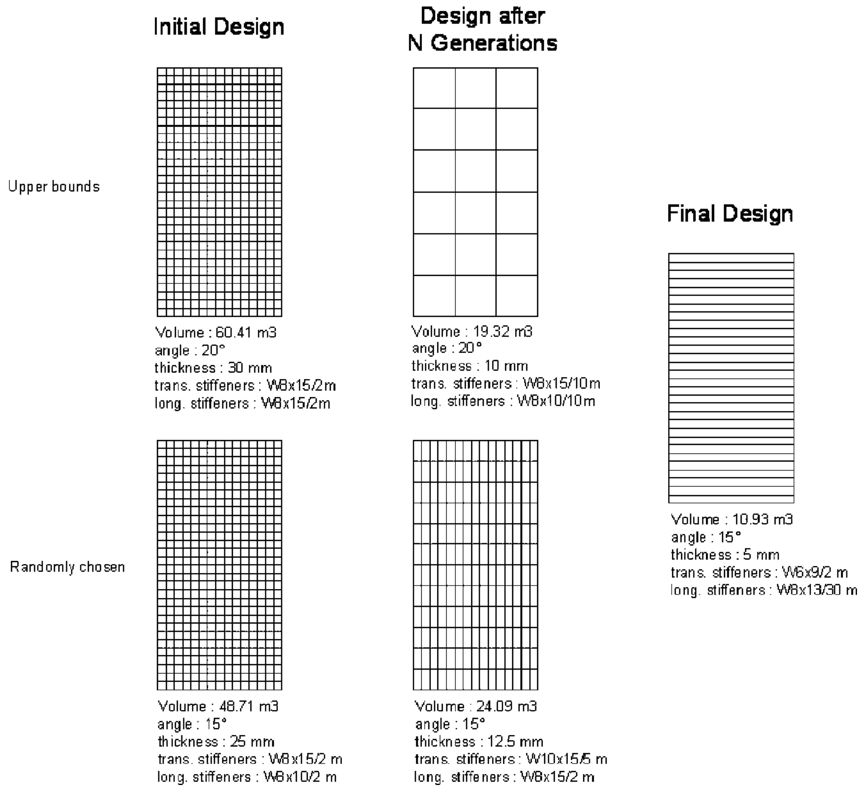

Fig. 1 Cylindrical roof: optimization process.

variables, the objective, and the constraint functions depend on the type of the application. However, most optimization problems can be expressed in standard mathematical terms as a nonlinear programming problem. A discrete structural optimization problem can be formulated in the following form:

$$\begin{aligned} &\text{minimize} && F(\boldsymbol{s}) \\ &\text{subject to} && g_j(\boldsymbol{s}) \leq 0, && j = 1, \ldots, m \\ & && s_i \in R^d, && i = 1, \ldots, n \end{aligned} \tag{1}$$

where $F(s)$ and $g_j(s)$ are the objective and constraints functions, respectively, and R^d is a given set of discrete values, whereas the design variables s_i, $i = 1, \ldots, n$, can take values only from this set.

There are three main classes of structural optimization problems depending on the type of the design variables used: sizing, shape, and topology. In sizing optimization problems, the aim is usually to minimize the weight of the structure under certain behavioral constraints on stresses and displacements. The design variables are most frequently chosen to be dimensions of the cross-sectional areas of the members of the structure. In structural shape optimization problems, the aim is to improve the performance of the structure by modifying its shape. The design variables are either some of the coordinates of the key points in the boundary of the structure or some other parameters that influence the shape of the structure. Structural topology optimization assists the designer to define the type of structure that is best suited to satisfy the operating conditions for the problem at hand. In the current study, topology optimization assists the designer to define the number and the position of the stiffening beams.

In addition to the three main classes of optimization problem, any combination of them can be implemented. In the present study, all three types of design variables have been combined. The aim is to minimize the weight of the structure under certain behavioral constraints. Sizing design variables are related to the definition of the cross section of the stiffeners and the thickness of the shell. The shape design variables control the inclination of the curved surface at the supports, whereas the topology design variables are related to the number and the position of the stiffeners in both the longitudinal and the transverse directions. These design variables may be active or nonactive, leading to a combined sizing–shape–topology optimization problem, when all design variables are active or to a sizing–shape optimization problem when only the sizing and shape design variables are active, etc. In Fig. 1, the optimization process corresponding to the second test example of Sec. VI for different initial designs is shown.

III. Solving the Optimization Problem

During the past three decades, many numerical methods have been developed to meet the demands of structural design optimization. These methods can be classified in two general categories: deterministic and probabilistic. Mathematical programming methods, and in particular the gradient-based optimizers that have been basically used for solving structural optimization problems in the past, belong to the first category of optimization algorithms. These methods make use of local curvature information, derived from linearization of the original functions by using their derivatives with respect to the design variables at points obtained in the process of optimization to construct an approximate model of the initial problem. Evolutionary algorithms (EA) are the most widely used class of methods of the second category. In particular, genetic algorithms (GA)[12] and ES[13] methods belong to EA class of methods and have been used in the past for solving structural optimization problems. These numerical algorithms imitate natural processes and are evolution-based systems maintaining a population of potential solutions. These systems employ some selection processes based on fitness of individuals and some recombination operators.

Gradient-based optimizers capture quickly the correct path toward the nearest optimum, irrespective of if it is a local or a global optimum, but it cannot assure that the global optimum can be found. On the other hand EA, due to their random search, are considered more robust in terms of global convergence; however, they may suffer from a slow rate of convergence toward the global optimum.[14] Another difference between EA and gradient-based optimizer is that EA are easily adapted to handle continuous, discrete, and mixed design variables.

In structural optimization problems, where the objective function and the constraints are highly nonlinear functions of the design variables, the computational effort spent in gradient calculations required by the mathematical programming algorithms is usually large. EA can be applied to any problem that can be formulated as a function optimization task.[15] In studies by Papadrakakis et al.[14] and Lagaros et al.,[16] it was found that probabilistic search algorithms are computationally efficient even if greater number of optimization cycles is needed to reach the optimum. These cycles are computationally less expensive than the corresponding cycles of mathematical programming algorithms because they do not need gradient evaluation. The selection of this optimization algorithm was based on the authors' as well as other researchers' experience regarding the relative superiority of ES over the rest of the methods in some specific problems.[14,17–19] The superiority of these methods, however, cannot be generalized.

A. Evolution Strategies

The ES can be divided into the two-membered evolution strategy (2-ES) and the multimembered evolution strategy (M-ES). The two-membered scheme is the minimal concept for an imitation of organic evolution. The two genetic operators of mutation and selection are taken as rules for variation of the parameters and for recursion of the iteration sequence, respectively. The 2-ES can be implemented in two steps:

Step 1 is mutation. The parent $s_p^{(g)}$ of the gth generation produces an offspring $s_o^{(g)}$, whose genotype is slightly different from that of the parent. Both parent and offspring vectors represent two-candidate optimum design vectors

$$s_o^{(g)} = s_p^{(g)} + z^{(g)} \tag{2}$$

where $z^{(g)}$ is a random vector.

Step 2 is selection. In this step, the best individual between the parent and the offspring is chosen to survive:

$$s_p^{(g+1)} = \begin{cases} s_o^{(g)} & \text{if } g_i\left(s_o^{(g)}\right) \le 0,\ i = 1, 2, \dots, l, \text{ and } f\left(s_o^{(g)}\right) \le f\left(s_p^{(g)}\right) \\ s_p^{(g)} & \text{otherwise} \end{cases} \tag{3}$$

The question of how to choose the random vector $z^{(g)}$ in step 1 is very important. This choice has the role of mutation, which is understood to be random, purposeless events that occur very rarely. In continuous optimization problems, the so-called $(0, \sigma_i)$ normal distribution is used to generate the vectors $z^{(g)}$ (Ref. 13).

The M-ES differ from the two-membered strategies in the size of the population and the additional genetic operator of recombination used. The two steps are defined as follows:

Step 1 is recombination and mutation. The population of μ parents of the gth generation produces λ offspring. For every offspring vector, a temporary parent vector $\tilde{s} = [\tilde{s}_1, \tilde{s}_2, \dots, \tilde{s}_n]^T$ is first built by means of recombination. From the temporary parent $\tilde{s}$, an offspring is being created in the same way as in the 2-ES [Eq. (2)].

Step 2 is selection. There are two different types of selection schemes employed by the M-ES:

1) The best μ individuals are selected from the population of $(\mu + \lambda)$ individuals, $(\mu + \lambda)$-ES.

2) The best μ individuals are selected from the population of $\lambda(\mu < \lambda)$ individuals, (μ, λ)-ES.

B. ES for Discrete Optimization Problems

In engineering practice, the design variables are not always continuous because the structural parts are usually constructed with a certain variation of their dimensions. Thus, design variables can only take values from a predefined discrete set. For the solution of discrete optimization problems, Cai and Thierauf[20] have proposed a modified ES algorithm. The basic differences between discrete and continuous ES are focused on the mutation and the recombination operators. New modified operators have to be engaged to assure that the generated design variables belong to the discrete design set. For discrete problems the following recombination scheme is used in the current study:

$$\tilde{s}_i = s_{a,i} \quad \text{or} \quad s_{b,i} \quad \text{randomly} \tag{4}$$

where $\tilde{s}_i$ is the ith component of the temporary parent vector $\tilde{s}$ and $s_{a,i}$ and $s_{b,i}$ are the ith components of the vectors s_a and s_b, which are two parent vectors randomly chosen from the population.

In the discrete version of ES the random vector $z^{(g)}$ is properly generated to force the offspring vector to move to another set of discrete values. These random vectors should follow the rule that large changes should rarely happen, whereas small changes occur more frequently. The variance of the random vector should be small, the difference between any two adjacent values, though, can be relatively large. For this reason, it is suggested that not all of the components of a parent vector, but only a few of them, for example, ℓ, should be randomly changed in every generation. In other words, the terms of vector $z^{(g)}$ are derived as follows:

$$z_i = \begin{cases} (\kappa + 1)\delta s_i, & \text{for} \quad \ell \text{ randomly chosen components} \\ 0, & \text{for} \quad n - \ell \text{ other components} \end{cases} \tag{5}$$

where δs_i is the difference between two adjacent values in the discrete set and κ is a random integer number that follows the Poisson distribution

$$p(\kappa) = [(\gamma)^\kappa / \kappa!] e^{-\gamma} \tag{6}$$

where γ is the standard deviation, as well as the mean value of the random number κ. The choice of ℓ depends on the size of the problem, and it is usually taken as one-fifth of the total number of design variables. The ℓ components of the temporary parent vector are selected using uniform random distribution.

C. Evolution Strategies for Structural Optimization Problems

The ES optimization algorithm starts with a set of parent vectors; if any of these parent vectors corresponds to an infeasible design, then this parent vector is modified until it becomes feasible. Subsequently, the offsprings are generated and checked if they are in the feasible region. The ES algorithm for structural optimization applications is an iterative process consisting of the following steps:

1) The selection step is selection of s_j, $j = 1, 2, \dots, \mu$, parent vectors of the design variables.

2) For the analysis step, solve $K(s_j)u_j = f$, $j = 1, 2, \dots, \mu$.

3) For the constraints check, all parent vectors become feasible.

4) For offspring generation, generate s_j, $j = 1, 2, \dots, \lambda$, offspring vectors of the design variables [Eqs. (2), (4), and (5)].

5) For the analysis step, solve $K(s_j)u_j = f$, $j = 1, 2, \dots, \lambda$.

6) For the constraints check, if satisfied continue, else go to step 4.

7) For the selection step, select the next generation parents according to $(\mu + \lambda)$ or (μ, λ) selection schemes.

8) For the convergence check, if satisfied stop, else go to step 4.

The procedure is terminated as soon as the mean value of the objective values from all parent vectors in the last $2 \cdot n \cdot \mu/\lambda$ generations has been improved by less than 0.01%.

IV. FE Formulation

An attempt to devise an efficient and robust shell finite element led Argyris et al. to the derivation of the TRIC shell element.[8] The formulation is based on the natural mode method.[21] TRIC is a shear-deformable facet shell element suitable for linear and nonlinear analysis of thin and moderately thick isotropic, as well as composite, plate and shell structures, and because of its natural formulation, it does not suffer from the various locking phenomena.[10] In this work, TRIC is used in the context of static analysis of isotropic shells, but laminate anisotropic shells can be analyzed in a similar fashion because the proposed methodology does not depend on the formulation of the FE problem. In conjunction with TRIC, the BEC[9] element is also used. BEC was originally proposed for laminate anisotropic beams and also can be combined with TRIC in a neat way due to the similarities on their formulations. It is shown elsewhere[9] that because of its formulation BEC is rendered with all of the advantages of TRIC. Both elements are considered reliable, accurate, and cost effective, as has been shown previously.[10,11] The basic features of TRIC and BEC elements are given in the Appendix.

V. Optimizing the Performance of Stiffened Shells

Shell structures, stiffened or nonstiffened, are very common in engineering practice because they combine high stiffening characteristics with low material volume. They are very common in civil, mechanical, naval, and aeronautical industries because they can span long and wide column-free spaces.

Cylindrical shells are perhaps the most useful shell structures because they lend themselves to relatively easy construction, while they can span large areas with a minimum of material. They are also very efficient because they use their shape to reduce stresses and thicknesses in the transverse direction. The procedure described can be easily expanded to cover a variety of applications where cross sections of different shapes, such as ellipse, parabola, or funicular curve, apart from the arced cross section of Figs. 2a and 2b, can be utilized.

To ensure that the performance of the shell meets the targets suggested by design code limit states, for example, serviceability limit state and ultimate limit state, the optimization process should consider the provisions set by the design code. For the purpose of this work, Eurocode standards are employed, although any design code can be implemented in a similar way. The loads used for the design of the case studies examined refer to the ultimate limit state according to Eurocode 1 (EC1).[22] Design code requirements are considered through the constraints of the optimization problem. Different constraint functions are used for the shell part of the structure and for the stiffening beams.

A. Shell

The von Mises yield criterion is employed to assess the value of an equivalent stress that will be compared with the yield stress f_y. Therefore, the following expression has to be satisfied for each triangular shell element:

$$\sqrt{\sigma_1^2 + \sigma_2^2 - 3\sigma_1\sigma_2 + 3\tau^2} \leq f_y/\gamma_{M0} \tag{7}$$

where σ_1, σ_2, and τ are the stresses in the middle surface x–y (Fig. 2c) of the triangle and γ_{M0} is a safety factor equal to 1.10.

B. Stiffening Beams

The constraint functions for beams subjected to biaxial bending under compression are given by the following formula of EC3[23]:

$$N_{sd}/(Af_y/\gamma_{M1}) + M_{sd,y}/(W_{pl,y}f_y/\gamma_{M1}) + M_{sd,z}/(W_{pl,z}f_y/\gamma_{M1}) \leq 1.0 \tag{8}$$

where N_{sd}, $M_{sd,y}$, $M_{sd,z}$ are the computed stress resultants, $W_{pl,y}$ and $W_{pl,z}$ are the plastic first moments of inertia, f_y is the yield stress, and γ_{M1} is a safety factor equal to 1.10. The upper flange of the beam cross section is assumed to be rigidly connected to the shell part of the structure, and therefore, longitudinal buckling is not developed in the stiffeners.

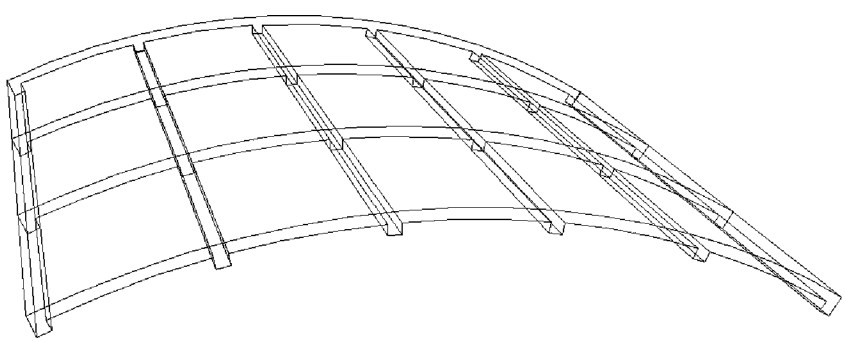

Fig. 2a Stiffened cylindrical roof.

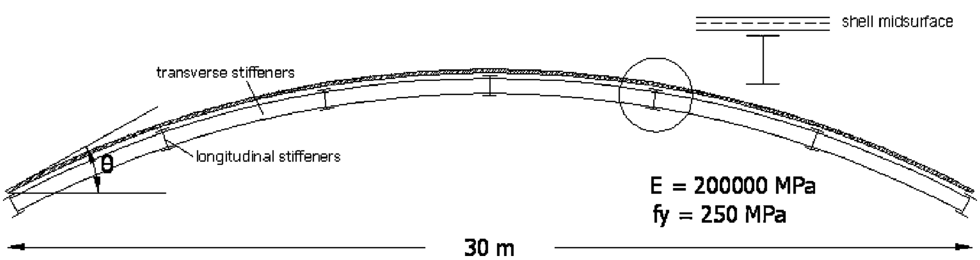

Fig. 2b Shell cross section.

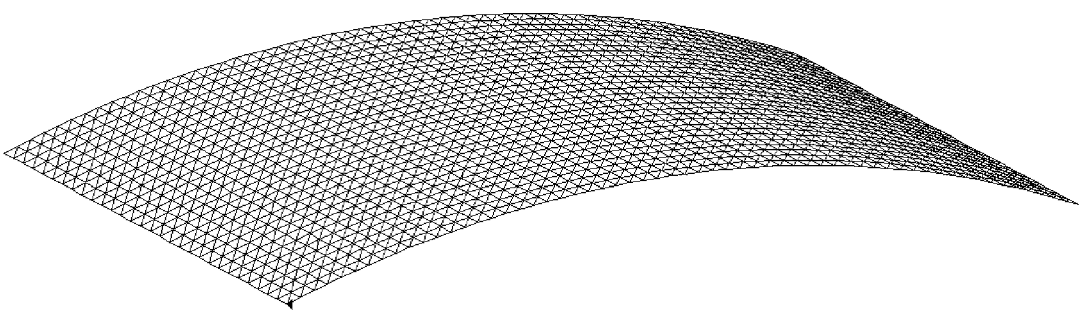

Fig. 2c Cylindrical roof FE mesh.

Table 1 Benchmark example, performance of various optimization algorithms

Method	Weight, kN	X_1, cm^2	X_2, cm^2	X_3, cm^2	X_4, cm^2	X_5, cm^2	X_6, cm^2	X_7, cm^2	X_8, cm^2	X_9, cm^2	X_{10}, cm^2
CONMIN[25]	24.75	145.16	12.19	160.45	102.13	0.65	11.29	108.13	127.29	135.35	16.19
OPTDYN[25]	24.34	165.81	0.65	162.00	125.10	0.65	0.65	99.35	131.10	133.81	7.35
LINRM[25]	27.80	139.16	70.84	142.45	96.45	0.65	70.84	122.00	118.84	118.71	87.16
SUMT[25]	26.39	198.00	15.29	204.00	75.23	0.65	23.94	140.06	134.84	90.13	21.03
M-3[25]	25.44	166.71	19.81	170.45	82.39	0.65	22.13	124.77	123.68	121.03	28.52
M-5[25]	25.47	166.64	18.58	170.64	82.26	0.65	24.32	124.97	123.74	121.10	28.26
GRP-UI[25]	25.47	159.87	26.90	159.87	93.23	0.65	26.90	112.64	124.26	124.32	33.94
GA[24]	24.97	216.13	10.45	141.94	100.00	10.45	10.45	91.61	128.39	128.39	16.90
GA[25]	24.28	216.13	10.45	141.94	91.61	10.45	10.45	51.42	147.74	141.94	10.45
GA[26]	24.23	216.13	10.45	141.94	89.68	10.45	10.45	51.42	147.74	147.74	10.45
ES (this work)	24.14	216.13	11.61	141.94	91.61	10.45	10.45	46.58	147.74	141.94	10.45

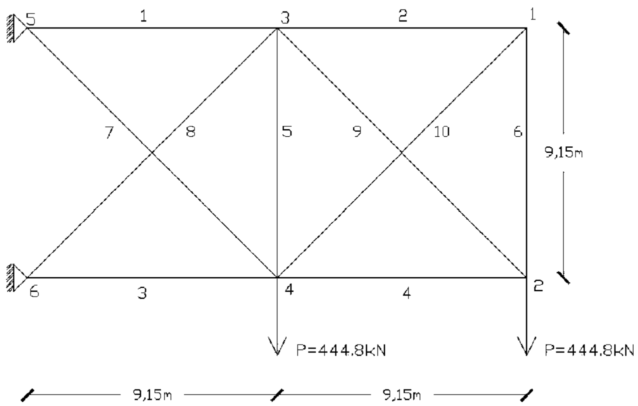

Fig. 3 Benchmark test example.

VI. Numerical Case Studies

In this study three numerical tests are examined. The first is a benchmark test example, where the efficiency of the optimization algorithm adopted is compared with a number of algorithms reported in the literature. To demonstrate the efficiency of the proposed methodology, two characteristic test examples are subsequently examined: a cylindrical shell and a storage silo. For each test example, a parametric study is performed, where different combinations of the active design variables are considered.

A. Benchmark Optimization Test

The first test example is the 10-bar truss[24–26] benchmark optimization problem shown in Fig. 3. Each member of the truss structure is considered as an independent design variable, and vertical downward loads of 444.8 kN at joints 2 and 4 are applied. A displacement constraint of 5.08 cm is enforced to nodes 2 and 4, and stress constraints are also enforced at each member of the structure with maximum tensile and compress stress equal to 172.4 MPa. The material used is aluminum, with modulus of elasticity of 68.9 GPa. The database of the discrete design variable is taken from the American Institute of Steel Construction (AISC). Thus, the double-angle profiles used are $A = (10.45\ 11.61\ 12.84\ 13.74\ 15.35\ 16.90\ 16.97\ 18.58\ 18.90\ 19.94\ 20.19\ 21.81\ 22.39\ 22.90\ 23.42\ 24.77\ 24.97\ 25.03\ 26.97\ 27.23\ 28.97\ 29.61\ 30.97\ 32.06\ 33.03\ 37.03\ 46.58\ 51.42\ 74.19\ 87.10\ 89.68\ 91.61\ 100.00\ 103.23\ 109.03\ 121.29\ 128.39\ 141.94\ 147.74\ 170.97\ 193.55\ 216.13)$ (cm^2). Table 1 gives the optimum results obtained. It can be seen that the weight of 5426.63 lb achieved by the ES outperforms all other optimization algorithms.

B. Cylindrical Shell

The case of a long (span/radius ratio greater than 5) stiffened and nonstiffened shell structure, shown in Fig. 2, spanning an area of 30×60 m^2 is considered. Shape optimization refers to the selection of the optimum curvature of the shell, which is defined by the angle θ as shown in Fig. 2b. Five discrete values, 0, 5, 10, 15, and 20 deg, of θ are considered. Topology optimization refers to the selection of the layout (position and number) of the stiffeners, which could be arranged every 2, 5, 10 and 30 m. Sizing optimization refers to the selection of the stiffener cross section and shell thickness. The sections are to be selected from the AISC tables of wide-flange sections, whereas the thickness of the shell is considered to be a continuous design variable taking values in the 2.5–30 mm range. To satisfy fabrication requirements, the stiffeners are set in one group with the same cross sections. In the transverse direction, the stiffeners are of arch shape, whereas in the longitudinal direction, they are straight lines. The shell discretization comprises 3422 TRIC elements with 10,080 degrees of freedom (DOF), whereas the beams are discretized with 116–1696 BEC elements, depending on the number of stiffeners used. The loads imposed are that of EC1 1) snow load S of magnitude 0.75 kN/m^2, 2) wind load W of magnitude 0.60 kN/m^2 acting upward, and 3) gravity load G, indicating the self-weight of the structure. Three ultimate limit-state combinations are considered:

$$1.35 \times G + 1.50 \times S$$

$$1.35 \times G + 1.50 \times W$$

$$1.35 \times (G + S + W) \tag{9}$$

A $(5 + 5)$ES optimization scheme is adopted for this test case, whereas two different initial populations of the design variables corresponding to the upper design values of the set and to randomly selected values are considered. A parametric study is carried out where four different combinations of active design variables of the cylindrical shell are examined: 1) without stiffeners (sizing–shape problem), 2) with stiffeners in the transverse direction only, free to move (sizing–shape–topology problem), 3) with stiffeners in the transverse direction only, fixed (sizing–shape problem), and 4) with stiffeners in both directions, free to move (sizing–shape–topology problem). In the first case, each design vector has two design variables corresponding to the angle θ (Fig. 2b) and the thickness of the shell. In the second case, each design vector has four design variables, those of the first case and also the stiffeners position and their cross section in the transverse direction. In the third case, the design variables are angle θ and the thickness and the cross section of the stiffeners. Finally, in the fourth case, each design vector has six design variables, those of the first two cases and two others corresponding to the stiffeners position and their cross section in the longitudinal direction. The four design cases examined and the corresponding design variables are summarized in Table 2. In Table 3, the initial randomly selected designs used, and their upper values are provided, whereas the iteration history of the value of the objective function at each FE analysis for the case of fixed stiffeners in the transverse direction is shown in Fig. 4.

The optimum design achieved for each case is summarized in Table 4. It can be seen that the optimum design obtained for each of the four cases does not depend on the values of the initial population. A substantial reduction on the total weight is observed when transverse stiffeners are considered, whereas longitudinal stiffeners contributed to a small additional reduction of the material volume. More specifically, a reduction of the volume of the order of 75%

Table 2 Design variables for each design case considered

Design case	Design variables					
	Shell curvature	Shell thickness	Stiffener position (transversally)	Stiffener cross section (transversally)	Stiffener position (longitudinally)	Stiffener cross section (longitudinally)
Without stiffeners	√	√				
Stiffeners free to move in transverse direction	√	√	√	√		
Stiffeners fixed in transverse direction	√	√		√		
Stiffeners free to move in both directions	√	√	√	√	√	√

Table 3 Cylindrical shell: initial designs

Initial design	Design variable	Volume, m^3
Without stiffeners, deg, mm		
Upper	20, 30	55.11
Random	20, 30	55.11
	15, 30	54.07
	15, 27.5	50.81
	20, 27.5	51.11
	20, 27.5	51.11
Stiffeners move in the transverse direction, deg, mm, m		
Upper	20, 30, $W_{8\times 15}/2$	57.83
Random	20, 30, $W_{8\times 15}/2$	57.83
	20, 30, $W_{6\times 15}/2$	57.32
	20, 30, $W_{6\times 15}/2$	57.32
	15, 30, $W_{6\times 15}/2$	48.22
	15, 30, $W_{6\times 15}/2$	48.22
Stiffeners fixed in the transverse direction, deg, mm, m		
Upper	20, 30, $W_{8\times 15}/4$	57.83
Random	20, 30, $W_{8\times 15}/4$	57.83
	20, 10, $W_{6\times 15}/4$	21.08
	15, 7.5, $W_{4\times 13}/4$	16.01
	15, 7.5, $W_{4\times 13}/4$	16.01
	15, 22.5, $W_{8\times 10}/4$	42.76
Stiffeners move in both directions, deg, mm, m, m		
Upper	20, 30, $W_{8\times 15}/2$, $W_{8\times 15}/2$	60.41
Random	20, 30, $W_{8\times 15}/2$, $W_{8\times 15}/2$	60.41
	15, 25, $W_{8\times 15}/10$, $W_{8\times 15}/2$	48.71
	15, 25, $W_{8\times 15}/10$, $W_{8\times 15}/2$	48.71
	15, 20, $W_{10\times 15}/2$, $W_{8\times 15}/10$	39.60
	20, 17.5, $W_{8\times 15}/10$, $W_{8\times 13}/10$	33.28

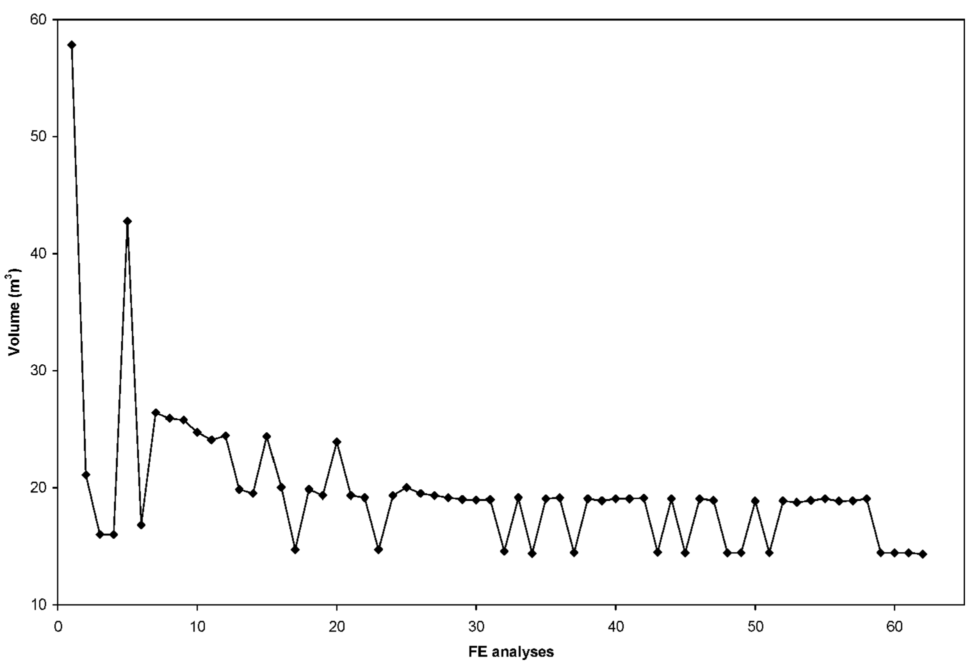

Fig. 4 Stiffened cylindrical roof: optimization history.

Table 4 Cylindrical shell: performance of discrete ES for the four test cases

Initial design	Optimum design	Generations	No. of FE analyses	Optimum volume, m^3	CPU time, s
Without stiffeners, deg, mm					
Upper	20, 25	2	31	45.92	203
Random	20, 25	7	23	45.92	149
Stiffeners move in the transverse direction, deg, mm, m					
Upper	15, 5, $W_{10\times12}/2$	59	203	11.35	1317
Random	15, 5, $W_{10\times12}/2$	38	131	11.35	849
Stiffeners fixed in the transverse direction, deg, mm, m					
Upper	20, 7.5, $W_{6\times9}/4$	42	127	14.62	825
Random	20, 7.5, $W_{6\times9}/4$	17	62	14.62	403
Stiffeners move in both directions, deg, mm, m, m					
Upper	15, 5, $W_{6\times9}/2$, $W_{8\times13}/30$	68	197	10.93	1278
Random	15, 5, $W_{6\times9}/2$, $W_{8\times13}/30$	24	86	10.93	560

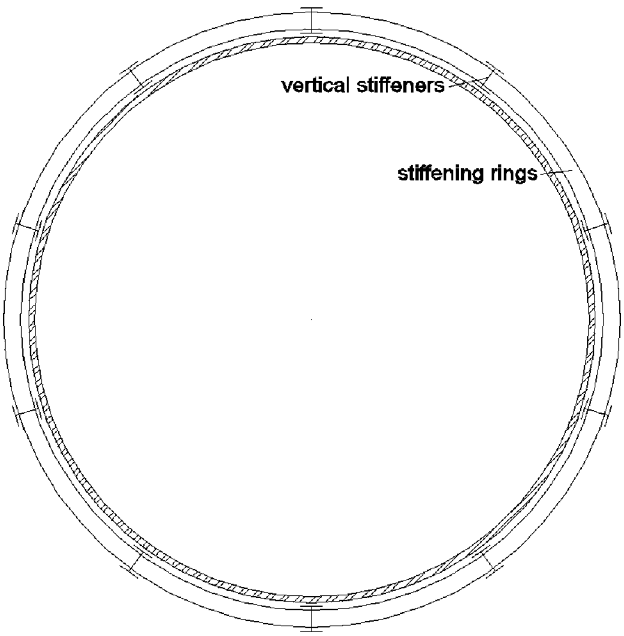

Fig. 5a Storage silo cross section.

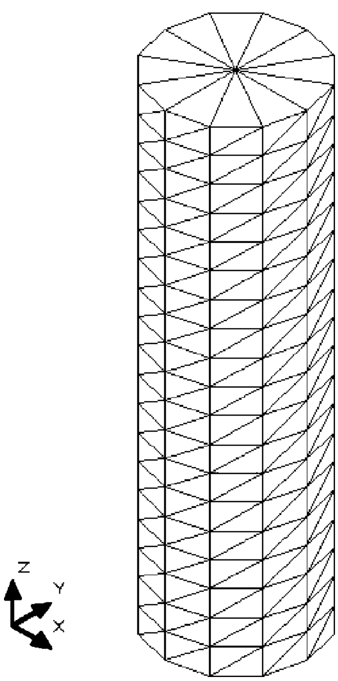

Fig. 5b Silo FE mesh.

Table 5 Storage silo: initial designs

Initial design	Design variable	Volume, m^3
Without stiffeners, mm		
Upper	30	12.80
Random	30	12.80
	27.5	11.73
	27.5	11.73
	25	10.67
	25	10.67
Stiffeners move in the vertical direction, mm, m		
Upper	30, $W_{8\times15}/1$	13.87
Random	30, $W_{8\times15}/1$	13.87
	27.5, $W_{6\times15}/1$	12.80
	25, $W_{6\times12}/5$	10.84
	15, $W_{6\times9}/1$	7.04
	15, $W_{4\times13}/2$	6.86
Stiffeners fixed every 5 m, mm, m		
Upper	30, $W_{8\times15}/5$	13.01
Random	30, $W_{8\times15}/5$	13.01
	27.5, $W_{6\times15}/5$	12.20
	25, $W_{8\times15}/5$	11.07
	27.5, $W_{6\times15}/5$	12.20
	27.5, $W_{10\times15}/5$	12.05
Stiffeners in both directions, mm, m		
Upper	30, $W_{8\times15}/1$, 16[$W_{8\times15}$]	14.56
Random	30, $W_{8\times15}/1$, 16[$W_{8\times15}$]	14.56
	20, $W_{8\times13}/1$, 16[$W_{8\times15}$]	10.05
	20, $W_{8\times13}/1$, 16[$W_{8\times15}$]	10.05
	15, $W_{6\times15}/1$, 8[$W_{12\times14}$]	7.81
	15, $W_{6\times15}/1$, 8[$W_{12\times14}$]	7.81

is achieved when stiffeners in both directions are considered as opposed to the nonstiffened case.

In Table 4, the CPU time required by the optimization procedure to reach the optimum design is also given. It can be seen that the required time is a few hundreds of seconds on a Pentium III 900-MHz processor, which is considered very satisfactory for this type of problem. This computational performance can be attributed to the optimization algorithm used, which allowed reaching the optimum design in a few tens of optimization steps.

C. Storage Silo

The storage silo of Fig. 5 with 20-m height and 6-m diam is examined. Material properties, cross section, and topology of the stiffeners are similar to those of the earlier example. The discretization of the shell structure comprises 480 TRIC elements with 1332 DOF, whereas the beams are discretized with 24–468 BEC elements, depending on the number of stiffeners used.

The loadings on the structure are the following: 1) snow load S of magnitude 0.75 kN/m^2, 2) wind load W of magnitude of 0.60 kN/m^2 acting downward, 3) gravity load G_{silo} consisting of the self-weight of the silo, 4) gravity load G_{mater} consisting of the weight of a

Table 6 Storage silo: performance of discrete ES for the four test cases

Initial design	Optimum design	Generations	No. of FE analyses	Optimum volume, m^3	CPU time, s
Without stiffeners, mm					
Upper	22.5	12	30	9.60	12
Random	22.5	8	24	9.60	9
Stiffeners move in the vertical direction, mm, m					
Upper	12.5, $W_{6\times 9}/10$	43	112	5.39	42
Random	12.5, $W_{6\times 9}/10$	16	37	5.39	14
Stiffeners fixed every 5 m, mm, m					
Upper	12.5, $W_{6\times 9}/10$	40	110	5.48	42
Random	12.5, $W_{6\times 9}/10$	12	36	5.48	14
Stiffeners move in both directions, mm, m					
Upper	12.5, $W_{6\times 9}/10$, $4[W_{8\times 13}]$	37	99	5.55	37
Random	12.5, $W_{6\times 9}/10$, $4[W_{8\times 13}]$	32	79	5.55	30

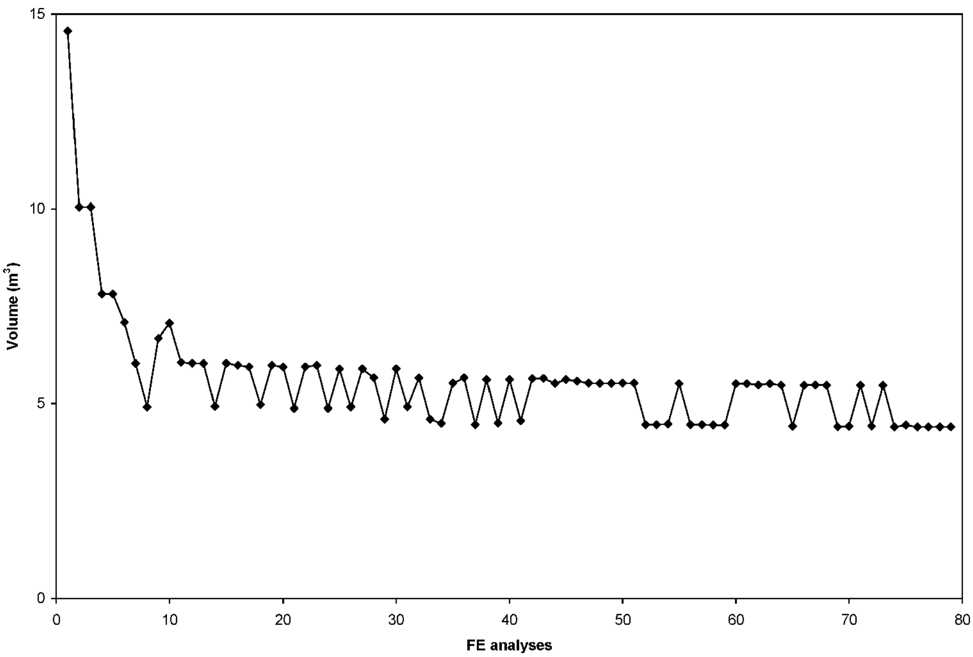

Fig. 6 Storage silo: optimization history.

contained material of specific weight equal to $\gamma = 16$ kN/m^3, and 5) pressure imposed during the evacuation of the silo, where a material magnification factor $C_h = 1.40$ is assumed (EC1, Part 4). Seven load combinations are considered for the design of the structure according to the provisions of EC1:

$$1.35 \times (G_{\text{silo}} + U) + 0.6 \times 1.5 \times (S)$$
$$1.35 \times (G_{\text{silo}} + U) + 0.6 \times 1.5 \times (W)$$
$$1.35 \times (G_{\text{silo}} + G_{\text{mater}}) + 0.6 \times 1.5 \times (S)$$
$$1.35 \times (G_{\text{silo}} + G_{\text{mater}}) + 0.6 \times 1.5 \times (W)$$
$$1.35 \times (G_{\text{silo}}) + 1.5 \times (S)$$
$$1.35 \times (G_{\text{silo}}) + 1.5 \times (W)$$
$$1.35 \times (G_{\text{silo}}) + (S) + (W) \tag{10}$$

The last three combinations correspond to an empty silo. All combinations define loading schemes for which the stress constraints of Eurocode are to be satisfied.

A $(5+5)$ES optimization scheme is adopted, and two different initial populations are used as before. Four design cases of the silo are examined: 1) without stiffeners (sizing problem), 2) with stiffeners along the vertical direction, free to move (sizing–topology problem), 3) with fixed stiffeners in the vertical direction every 5 m fixed, and 4) with stiffeners along both directions, free to move (sizing–topology problem) having one, three, and five design variables, respectively. The initial randomly selected designs and their upper values are listed in Table 5, whereas the iteration history of the value of the objective function at each FE analysis for the case of stiffeners varying in both directions is shown in Fig. 6.

Table 6 presents the performance of the optimization procedure for each case examined. The results obtained follow the same trend as in the earlier example. It can be seen that a reduction of the volume of the order of 40% was achieved when stiffeners in both directions are considered, as opposed to the nonstiffened case. The computational performance is related in a straightforward manner to the number of optimization steps and the size of the FE simulation. The optimization steps are more or less similar to those required in the preceding example, whereas, due to the coarser FE mesh, the total computing time required is about one order of magnitude less than the corresponding times required for the cylindrical shell.

VII. Conclusions

A design methodology of stiffened shells that combines stiffening topology with shape and sizing optimization has been proposed in this paper. The optimization procedure implemented, combined with cost-effective and accurate FE simulation of shell and stiffening beams, resulted in a robust and efficient optimization tool that can be used for the optimum design of real-world stiffened shell structures of any size, type, and configuration. The beneficial effect of transverse stiffeners on the performance of shell structures and the substantial reduction on material volume achieved were demonstrated and assessed quantitatively. The optimization of stiffened shells was carried out by using evolution strategies and, in particular, their mixed-discrete version. With relatively few FE analyses, the ES algorithm implemented can reach the optimum design regardless of the type of the optimization problem. The FE simulation adopted with the combination of TRIC–BEC elements for the simulation of shell and beam stiffeners can contribute further in the reduction of the computational cost.

Appendix: Natural Elements TRIC and BEC

The formulation of the beam and the shell FE is presented. It is assumed that the centroidal axis of the beam elements coincides with the corresponding midsurface axis of the shell elements.

A. TRIC Shell Element

TRIC is a multilayered triangular shell element. Four coordinate systems are adopted, namely, the material, the natural, the local, and the global coordinate system. The stiffness is contributed by deformations only and not by the associated rigid-body motions. The element has 18 DOF (6 per node), and hence, 12 natural straining modes are defined. Three natural axial strains γ_t and natural transverse shear strains γ_s are measured parallel to the edges of the triangle. The axial strains γ_t are related to the three in-plane local Cartesian strains γ' according to

$$\gamma_t = B^T\gamma' \Leftrightarrow \begin{Bmatrix}\gamma_{t\alpha}\\ \gamma_{t\beta}\\ \gamma_{t\gamma}\end{Bmatrix} = \begin{bmatrix} c^2_{\alpha x'} & s^2_{\alpha x'} & \sqrt{2}s_{\alpha x'}c_{\alpha x'}\\ c^2_{\beta x'} & s^2_{\beta x'} & \sqrt{2}s_{\beta x'}c_{\beta x'}\\ c^2_{\gamma x'} & s^2_{\gamma x'} & \sqrt{2}s_{\gamma x'}c_{\gamma x'}\end{bmatrix}\begin{Bmatrix}\gamma_{x'x'}\\ \gamma_{y'y'}\\ \sqrt{2}\gamma_{x'y'}\end{Bmatrix} \tag{A1}$$

where $c_{ix'}$ and $s_{ix'}$ are the cosine and the sine of the angle between the i side of the triangle and the local x axis. A similar expression can be derived for the transverse shear strains. The constitutive relations are established through the following transformations:

material system → local system → natural system

The corresponding natural stresses σ_c and the natural transverse shear stresses σ_s are obtained following a series of calculations[9]:

$$\begin{Bmatrix}\sigma_c\\ \sigma_s\end{Bmatrix}_r = \begin{bmatrix}\kappa_{ct} & \cdot\\ \cdot & \chi_s\end{bmatrix}_r \begin{Bmatrix}\gamma_t\\ \gamma_s\end{Bmatrix}_r \tag{A2}$$

for each layer r. Matrices κ_{ct} and χ_s are constitutive matrices. The natural stiffness matrix can be produced from the statement of variation of the strain energy with respect to the natural coordinates:

$$\left.\begin{array}{l}\delta U = \displaystyle\int_V \sigma_c^T\delta\gamma_t\,\mathrm{d}V \xrightarrow{(A2)} \delta U = \int_V \gamma_t^T\kappa_{ct}\delta\gamma_t\,\mathrm{d}V\\ \qquad\qquad \gamma_t = \alpha_N\rho_N\end{array}\right\}$$

$$\rightarrow \delta U = \rho_N^T\left[\int_V \alpha_N^T\kappa_{ct}\alpha_N\,\mathrm{d}V\right]\mathrm{d}\rho_N \tag{A3}$$

where ρ_N is the vector of the natural straining modes. Transformations are subsequently initiated to obtain the natural matrix first to the local and then to the global coordinate system, where $\rho = \bar{\alpha}_N\rho_N$,

$$\delta U = \rho^T \underbrace{\left[T_{06}^T \underbrace{\left[\bar{\alpha}_N^T \underbrace{\left[\int_V \alpha_N^T\kappa_{ct}\alpha_N\,\mathrm{d}V\right]}_{\text{stiffness natural coord. }(12\times 12)} \bar{\alpha}_N\right]}_{\text{stiffness local coord. }(18\times 18)} T_{06}\right]}_{\text{stiffness global coord. }(18\times 18)} \rho \tag{A4}$$

ρ is the vector of Cartesian displacements in the global system, whereas T_{06}, $\bar{a}_N$, and a_N are transformation matrices. More details on the formulation of TRIC may be found in Ref. 8.

B. BEC Element

The four coordinate systems described for the TRIC element also apply for BEC. Each node has six DOF, whereas the derivation of the stiffness matrix is based on similar concepts as TRIC. Six natural straining modes are employed, whereas an explicit relation between them and the strain vector is established:

$$\gamma = \alpha_N\rho_N \Leftrightarrow \begin{bmatrix}\gamma_{xx}\\ \sqrt{2}\gamma_{xy}\\ \sqrt{2}\gamma_{xz}\end{bmatrix}$$

$$= \frac{1}{l}\begin{bmatrix} 1 & z & -3z\zeta & y & -3y\zeta & \cdot\\ \cdot & \cdot & \cdot & \cdot & \cdot & \dfrac{1}{\sqrt{2}}\left(\dfrac{\partial\Psi(y,z)}{\partial y} - z\right)\\ \cdot & \cdot & \cdot & \cdot & \cdot & \dfrac{1}{\sqrt{2}}\left(\dfrac{\partial\Psi(y,z)}{\partial z} + y\right)\end{bmatrix}\begin{bmatrix}\rho_{N1}\\ \rho_{N2}\\ \rho_{N3}\\ \rho_{N4}\\ \rho_{N5}\\ \rho_{N6}\end{bmatrix} \tag{A5}$$

where ζ is the nondimensional natural coordinate along the element and $\Psi(y,z)$ is the warping function. The stiffness matrix for each element in the global system is formulated through the expression, where $\rho = \bar{\alpha}_N\rho_N$,

$$\delta U = \rho^T \underbrace{\left[T_{04}^T \underbrace{\left[\bar{\alpha}_N^T \underbrace{\left[\int_V \alpha_N^T\kappa\alpha_N\,\mathrm{d}V\right]}_{\text{stiffness natural coord. }(6\times 6)} \bar{\alpha}_N\right]}_{\text{stiffness local coord. }(12\times 12)} T_{04}\right]}_{\text{stiffness global coord. }(12\times 12)} \rho \tag{A6}$$

$\bar{a}_N$ is a transformation matrix, κ is the constitutive matrix, and T_{04} is the matrix of direction cosines. More details on the formulation may be found in Ref. 9.

References

[1] Maute, K., and Ramm, E., "Adaptive Topology Optimization of Shell Structures," *AIAA Journal*, Vol. 35, No. 11, 1997, pp. 1767–1783.

[2] Lee, S. J., Bae, J. E., and Hinton, E., "Shell Topology Optimization Using the Layered Artificial Material Model," *International Journal for Numerical Methods in Engineering*, Vol. 47, No. 4, 2000, pp. 843–868.

[3] Magnucki, K., "Optimal Design of a Horizontal Circular Tank with Ellipsoidal Heads," *Journal of Structural Multidisciplinary Optimization*, Vol. 16, 1998, pp. 226–229.

[4] Afonso, S. B., Belbidia, F., Hinton, E., and Antonino, G. R., "A Combined Structural Topology and Sizing Optimization Procedure for Optimum Plates Design," *Proceedings of the European Congress on Computational Methods in Applied Sciences and Engineering on Disc* [CD-ROM], CIMNE, Barcelona, 2000.

[5] Akl, W., Ruzzen, M., and Baz, A., "Optimal Design of Underwater Stiffened Shells," *Journal of Structural Multidisciplinary Optimization*, Vol. 23, 2002, pp. 297–310.

[6] Farkas, J., and Jarmai, K., "Optimum Design of Welded Stiffened Plates Loaded by Hydrostatic Normal Pressure," *Journal of Structural Multidisciplinary Optimization*, Vol. 20, 2000, pp. 311–316.

[7] Butler, R., Lillico, M., Hunt, G. W., and McDonald, N. J., "Experiments on Interactive Buckling in Optimized Stiffened Panels," *Journal of Structural Multidisciplinary Optimization*, Vol. 23, 2001, pp. 40–48.

[8] Argyris, J. H., Tenek, L., and Olofsson, L., "TRIC: A Simple But Sophisticated 3-Node Triangular Element Based on 6 Rigid Body and 12 Straining Modes for Fast Computational Simulations of Arbitrary Isotropic and Laminated Composite Shells," *Computer Methods in Applied Mechanics and Engineering*, Vol. 145, 1997, pp. 11–85.

[9]Argyris, J. H., Tenek, L., and Mattssonn, A., "BEC: A 2-Node Fast Converging Shear-Deformable and Composite Beam Element Based on 6 Rigid-body and 6 Straining Modes," *Computer Methods in Applied Mechanics and Engineering*, Vol. 152, 1998, pp. 281–336.

[10]Argyris, J. H., Papadrakakis, M., Apostolopoulou, C., and Koutsourelakis, S., "The TRIC Shell Element: Theoretical and Numerical Investigation," *Computer Methods in Applied Mechanics and Engineering*, Vol. 182, No. 1-2, 2000, pp. 217–245.

[11]Argyris, J., Tenek, L., Papadrakakis, M., and Apostolopoulou,C., "Post-bucking Performance of the TRIC Natural Mode Triangular Element for Isotropic and Laminated Composite Shells," *Computer Methods in Applied Mechanics and Engineering*, Vol. 166, 1999, pp. 211–231.

[12]Goldberg, D. E, *Genetic Algorithms in Search, Optimization and Machine Learning*, Addison-Wesley, Reading, MA, 1989.

[13]Schwefel, H. P., *Numerical Optimization for Computer Models*, Wiley, Chichester, England, U.K., 1981.

[14]Papadrakakis, M., Tsompanakis, Y., and Lagaros, N. D., "Structural Shape Optimization Using Evolution Strategies," *Engineering Optimization Journal*, Vol. 31, 1999, pp. 515–540.

[15]Fogel, D. B., "An Introduction to Evolutionary Computation and Some Applications," *Evolutionary Algorithms in Engineering and Computer Science*, edited by K. Miettinen, M. M. Mukela, P. Neittaanmaki, and J. Periaux, Wiley, Chichester, England, U.K., 1999, pp. 23–41.

[16]Lagaros, N. D., Papadrakakis, M., and Kokossalakis, G., "Advances in Structural Optimization with Evolutionary Algorithms," *Computer and Structures*, Vol. 80, No. 7-8, 2002, pp. 571–587.

[17]Bäck, T., Rudolph, G., and Schwefel, H. P., "Evolutionary Programming and Evolution Strategies: Similarities and Differences," *Proceedings of the Second Annual Conference on Evolutionary Programming*, edited by D. B. Fogel and W. Atmar, Evolutionary Programming Society, San Diego, CA, 1993, pp. 11–22.

[18]Hoffmeister, F., and Bäck, T., "Genetic Algorithms and Evolution Strategies: Similarities and Differences," Systems Analysis Research Group, Dept. of Computer Science, Rept. TR-SYS-1/92, Univ. of Dortmund, Dortmund, Germany, Oct. 1992.

[19]Bäck, T., and Schwefel, H.-P., "An Overview of Evolutionary Algorithms for Parameter Optimization," *Journal of Evolutionary Computation*, Vol. 1, No. 1, 1993, pp. 1–23.

[20]Cai, J., and Thierauf, G., "Discrete Structural Optimization Using Evolution Strategies," *Neural Networks and Combinatorial in Civil and Structural Engineering*, edited by B. H. V. Topping and A. I. Khan, Civil-Comp, Ltd., Edinburgh, 1993, pp. 95–100.

[21]Argyris, J. H., Balmer, H., Doltsinis, J. St., Dunne, P. C., Haase, M., Muller, M., and Scharpf, W. D., "Finite Element Method—The Natural Approach," *Computer Methods in Applied Mechanics and Engineering*, Vol. 17/18, 1979, pp. 1–106.

[22]"Eurocode 1: Actions on Structures, Part 1.1: Densities, Self-Weight and Imposed Loads for Buildings; Part 1.3: Snow Loads; Part 1.4: Wind Loads," European Committee for Standardization, Brussels, Jan. 1991.

[23]"Eurocode 3: Design of Steel Structures, Part 1.1: General Rules; Part 1.5: Strength and Stability of Planar Plated Structures Without Transverse Loading," European Committee for Standardization, Brussels, Jan. 1993.

[24]Rajeev, S., and Krishnamoorty, C. S., "Discrete Optimization of Structures Using Genetic Algorithms," *Journal of Structural Engineering*, Vol. 118, 1992, pp. 1233–1250.

[25]Galante, M., "Genetic Algorithms as an Approach to Optimize Real-Word Trusses," *International Journal for Numerical Methods in Engineering*, Vol. 39, 1996, pp. 361–382.

[26]Ghasemi, M. R., and Hinton, E., "Truss Optimization Using Genetic Algorithms," *Journal of Engineering Computations*, Vol. 16, No. 3, 1999, pp. 272–301.

A. Messac
Associate Editor